Journal of Power Sources 203 (2012) 243–249

Contents lists available at SciVerse ScienceDirect

Journal of Power Sources

journal homepage: www.elsevier.com/locate/jpowsour

# Reduced graphene oxide–nickel oxide composite as high performance electrode materials for supercapacitors

Xianjun Zhu*, Huaili Dai, Jing Hu, Lei Ding, Li Jiang

*College of Chemistry, Central China Normal University, Wuhan, Hubei 430079, China*

ARTICLE INFO

*Article history:*
Received 11 September 2011
Received in revised form 19 October 2011
Accepted 18 November 2011
Available online 30 November 2011

*Keywords:*
Reduced graphene oxide
Nickel oxide
Supercapacitors
Homogeneous coprecipitation

ABSTRACT

Reduced graphene oxide and NiO composite is prepared by homogeneous coprecipitation and subsequent annealing. Characterizations show that NiO particles have a nanosheet-based microsphere structure and anchor uniformly on the surface of reduced graphene oxide platelets. The RG-O/NiO-based supercapacitors exhibit high specific capacitance of 770 F $g^{-1}$, and enhanced rate capability. It is found that the electrochemical performance can be enhanced by anchoring NiO particles on the surface of RG-O platelets in the RG-O/NiO composite. This method provides a facile and straightforward approach to distribute NiO nanoparticles onto the surface of RG-O sheets and can be extended to the preparation of other RG-O/metal oxides composite for electrochemical energy storage.



## 1. Introduction

Electrochemical supercapacitors are considered as a promising candidate for energy storage and conversion devices due to high power performance, long cyclic life, and low maintenance cost [1–3]. Great efforts have been made to improve their performance by developing different electrode materials such as various forms of carbon, conducting polymers and transition metal oxides [4,5]. Based on the electrode materials, there are two kinds of supercapacitors: (1) double-layer capacitance arising from the charge separation at the electrode/electrolyte interface and (2) pseudocapacitance arising from fast, reversible Faradaic reactions occurring at or near a solid electrode surface.

Various forms of carbonaceous materials, such as active carbons, carbon fibers, and CNTs, have been investigated as the electrode materials for electrochemical double layer capacitors [6,7]. Graphene, with a unique two-dimensional structure, is predicted to be an excellent electrode material for energy storage and conversion system due to its large surface area, high electrical conductivity, flexibility, and mechanical strength [8,9]. Recently, it has been proposed that graphene should be a competitive material for supercapacitor applications [10]. However, the effective surface area of graphene materials should depend highly on the layers. That is to say, single or few layered graphene with less agglomeration should be expected to have higher effective surface area and thus better supercapacitor performance [11–13].

On the other hand, transition metal oxides, such as $RuO_2$, exhibit good pseudocapacitance performance and are promising materials for pseudocapacitors [4,14]. But the high cost of these materials limits their commercialization. As a potential electrode material for the replacement of $RuO_2$ in pseudocapacitors, NiO has exhibited distinguished properties due to its good supercapacitor behavior, environmental compatibility, and cost effectiveness [15,16]. However, the specific capacitance of NiO is much lower than its theoretical value (ca. 2573 F $g^{-1}$ within 0.5 V), depending on its synthesis method and conductivity of NiO electrodes [17,18]. In order to utilize both Faradaic and non-Faradaic processes for large capacity-charge storage, various NiO/carbon composites were explored as electrode materials for hybrid supercapacitors [19–22]. Recent works have shown some transition metal oxides coupled with reduced graphene oxide for supercapacitor applications [23,24]. It was found that the loading of fine metal oxide particles can avoid or decrease the possibility of serious agglomeration and restacking of graphene ensembles, and consequently provide a higher available electrochemically active surface area, resulting in a higher electrochemical performance by exploiting the full advantages of graphene-based double layer capacitance and metal-oxide-based pseudocapacitance. Therefore, a method to prepare the composite materials in which metal oxide particles are uniformly distributed in the 'graphene' matrix still remains a challenge.

Herein, we report a simple method for obtaining a composite consisting of nanosheet-based NiO microspheres decorating

* Corresponding author. Tel.: +86 27 67868388.
*E-mail address:* xianjunzhu@yahoo.com.cn (X. Zhu).

0378-7753/$ – see front matter © 2011 Elsevier B.V. All rights reserved.
doi:10.1016/j.jpowsour.2011.11.055

reduced graphene oxide (RG-O) platelets, what we hereafter refer to as the "RG-O/NiO". The process involves homogeneous coprecipitation of $NiCl_2$ in a suspension of graphene oxide (G-O) platelets using urea and subsequent reduction of the G-O with hydrazine by refluxing to yield RG-O platelets decorated with $Ni(OH)_2$ nanoparticles, and finally annealing at 400 °C for 3 h under a nitrogen atmosphere with the aim of obtaining NiO particles. As an electrode material for electrochemical supercapacitors, it can deliver 770 F $g^{-1}$ specific capacitance. Our synthesis method presents a promising general route for the large-scale production of metal oxide particles/RG-O platelet composites as energy storage materials.

## 2. Experimental

### 2.1. Synthesis of graphite oxide

Graphite oxide was synthesized from natural graphite powders (500 mesh, Sinopharm Chemical Reagent Co., Ltd.) by a modified Hummers method [25]. Typically, graphite powders (2 g) and $NaNO_3$ (1 g; >99%) were mixed, then put into concentrated $H_2SO_4$ (96 ml; 98%) in an ice bath. Under vigorous stirring, $KMnO_4$ (6 g; 99.5%) was gradually added and the temperature of the mixture was kept below 20 °C. After removing the ice bath, the mixture was stirred at 35 °C in a water bath for 4 h. As the reaction progressed, the mixture became pasty with a brownish color. 150 ml $H_2O$ was then slowly added to the pasty mixture. Because large amounts of heat were generated by addition of water into the concentrated $H_2SO_4$ medium, water should be added slowly and at the same time keeping the mixture in an ice bath to maintain the temperature below 50 °C. After dilution with 240 ml $H_2O$, 5 ml of 30% $H_2O_2$ (Sinopharm Chemical Reagent Co., Ltd.) was added to the mixture, and the color of this diluted solution became a brilliant yellow. After continuously stirring for 2 h, the mixture was filtered and washed with 10% HCl (250 ml), then DI water and then anhydrous ethanol to remove other ions. Finally, the resulting solid was dried under vacuum.

### 2.2. Preparation of RG-O/NiO composite

The RG-O/NiO composite was prepared by homogeneous coprecipitation and subsequent reduction with hydrazine by refluxing. In a typical experiment, 5 mmol $NiCl_2$ (0.65 g; >98%) was dissolved in 50 ml water, 150 mmol urea (9.0 g; 99%) was dissolved in another 50 ml water, then urea and $NiCl_2$ solutions were slowly and sequentially added to 50 ml of 1 mg $ml^{-1}$ graphite oxide suspension under stirring. After exposure to ultrasound from an ultrasonic bath for 30 min, the mixture was heated at 90 °C for 1.5 h. When cooled to room temperature, 0.5 ml $N_2H_4$ (85%, Sinopharm Chemical Reagent Co., Ltd.) was added to the mixture while it was stirred. Then the mixture was refluxed at 100 °C for 24 h in an oil bath, during which the mixture color changed from black-brown to black. Then, the black mixture was collected by filtration. After washing with DI water in an attempt to remove any excess hydrazine as well as other ions, the as-prepared product was annealed at 400 °C for 3 h under an atmosphere of nitrogen in order to obtain a RG-O/NiO composite. For comparison, NiO without RG-O was also synthesized using the same procedure.

### 2.3. Characterization

The structure of the as-prepared RG-O/NiO composite was characterized by X-ray diffraction (XRD, CuKα radiation; λ = 1.5414 Å). Scanning electron microscopy (SEM) was performed using JSM-6700F (5 kV). Transmission electron microscopy (TEM, JEM-2010FEF; 200 keV) was used to study the morphology and microstructure of the composites. Raman spectrum measurements were carried out using INVIA (RENISHAW, England) system with a 514.5-nm wavelength incident laser light. Thermal gravimetric analysis (TGA) was measured with a SDT600 apparatus using a heating rate of 5 °C $min^{-1}$ under 20 ml $min^{-1}$ of flow air.

### 2.4. Electrochemical characterization

The working electrode was prepared as follows. The RG-O/NiO composite and polytetrafluoroethylene (PTFE) were mixed in a mass ratio of 95:5 in an agate mortar, rolled the mixture into thin sheet, and then punched out several pieces of 15 mm diameter discs. Following, the discs were pressed onto the nickel foam substrate (16 mm) under 10 MPa pressure. The mass of each electrode was ~4 mg.

Electrochemical measurements were carried out by a three-electrode cell, in which platinum net was used as counter electrode and Hg/HgO (in 6 M KOH) as reference electrode. The electrolyte was 6 M KOH aqueous solution. Cyclic voltammograms (CVs) were done between 0 and 0.55 V (vs. Hg/HgO) at different scan rates using CHI650A (Shanghai CH Instrument Company, China). Galvanostatic charge/discharge curves were measured in the potential range of 0–0.50 V (vs. Hg/HgO) by a Land battery tester (2001A, Wuhan Jinnuo Instrument Company, China). The specific capacitance of the electrode was calculated from the CV curves according to $C = \int Idt/(m\Delta V)$, where $I$ is the oxidation or reduction current, $dt$ is time differential, $m$ indicates the mass of active material, and $\Delta V$ indicates the voltage range of one sweep segment. Specific capacitance could also be calculated from the galvanostatic charge and discharge curves, using the equation $C = I\Delta t/(m\Delta V)$, where $I$ is charge or discharge current, $\Delta t$ is the time for a full charge or discharge, m indicates the mass of active material, and $\Delta V$ represents the voltage change of a full charge or discharge.

## 3. Results and discussion

As shown in Scheme 1, graphite oxide prepared by a modified Hummers method, was sonicated in water to form a suspension of G-O platelets. For the synthesis of the RG-O/NiO composite, $NiCl_2$ was hydrolyzed in the graphene oxide suspension in the presence of urea at 90 °C for 1.5 h in an oil bath. The molar ratio of $NiCl_2$ to urea was 1:30. This step yielded a uniform $Ni(OH)_2$ coating on the surface of the graphene oxide platelets. During hydrolysis, urea releases hydroxyl ions slowly and uniformly in the suspension, resulting in the formation of $Ni(OH)_2$ as suggested by the following reactions:

$$CO(NH_2)_2 + 3H_2O \rightarrow 2NH_4^+ + CO_2 + 2OH^- \quad (1)$$

$$Ni^{2+} + 2OH^- \rightarrow Ni(OH)_2 \quad (2)$$

The $Ni(OH)_2$ particles produced likely anchor onto the surface of the G-O platelets through oxygen-containing functional groups, such as hydroxyl, epoxyl, and carboxyl.

After the suspension was cooled to room temperature, a trace amount of hydrazine was added to the suspension under continuous stirring and the suspension was refluxed at 100 °C for 24 h in an oil bath, during when G-O gets converted to RG-O. After filtration, the as-obtained sample was annealed at 400 °C for 3 h under a nitrogen atmosphere; $Ni(OH)_2$ decomposes to yield NiO particles following $Ni(OH)_2 \rightarrow NiO + H_2O$. As characterized by X-ray diffraction (XRD), the as-prepared composite has the characteristic peaks of NiO (JCPDS: 65-2901) and RG-O (see FS. 1), indicating that the as-prepared product is composed of NiO and RG-O. The Raman spectrum also shows characteristic peaks of NiO as well as the D and G characteristic peaks of RG-O (see FS. 2). The composite contains 10 wt% RG-O as measured by thermal gravimetric analysis (see FS. 3).

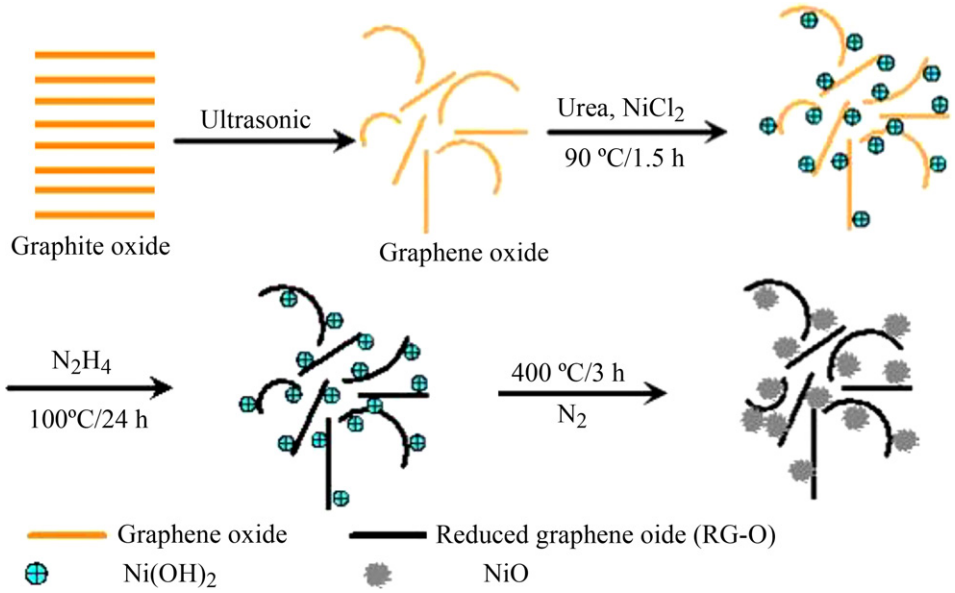


**Scheme 1.** Schematic illustration for the synthesis of RG-O/NiO.

The morphology of the RG-O/NiO composite was studied by scanning electron microscopy (SEM) as shown in Fig. 1. It can be seen from Fig. 1a and b that RG-O/NiO composite consists of thin, crumpled RG-O platelets closely connecting with each other to form a 3D network structure. NiO particles were distributed on the curved RG-O platelets. It can be seen from SEM that these NiO particles are nanosheet-based sphere-like structures. The morphology of NiO particles can also be seen from TEM images of RG-O/NiO

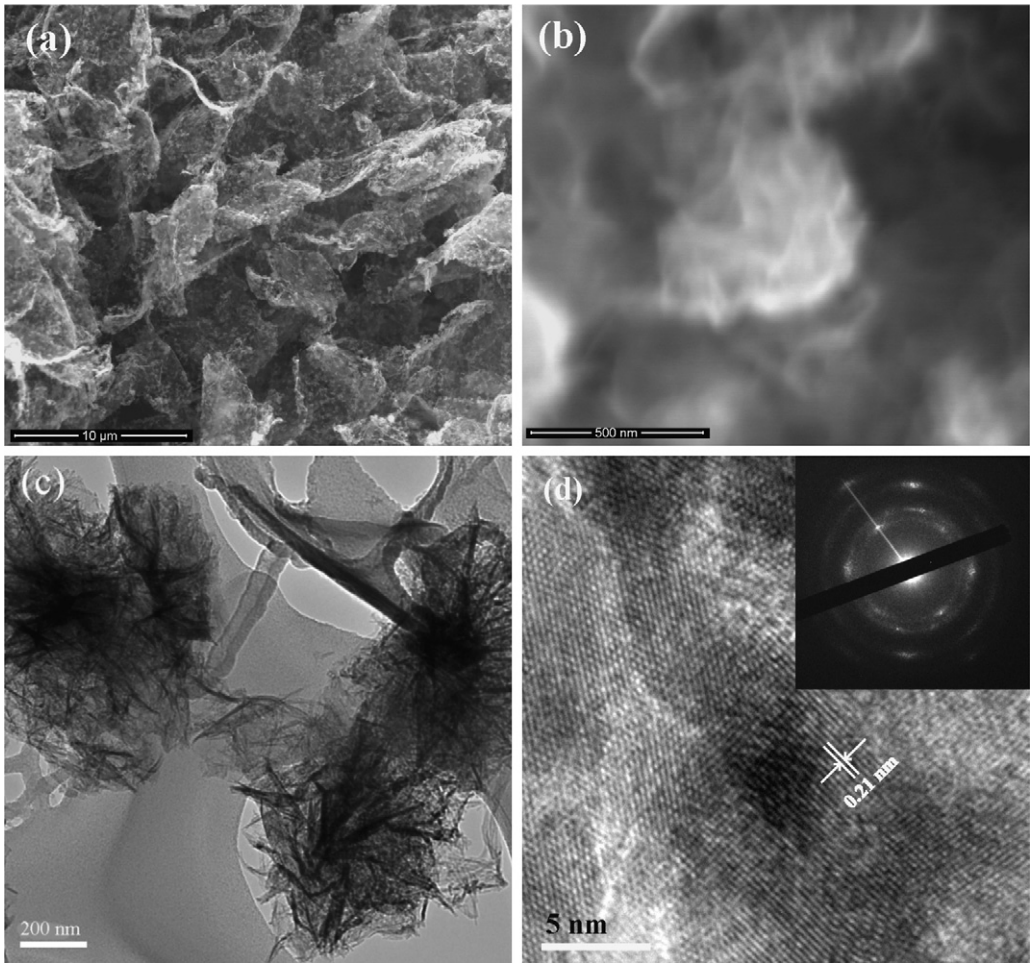


**Fig. 1.** SEM and TEM images of the RG-O/NiO.

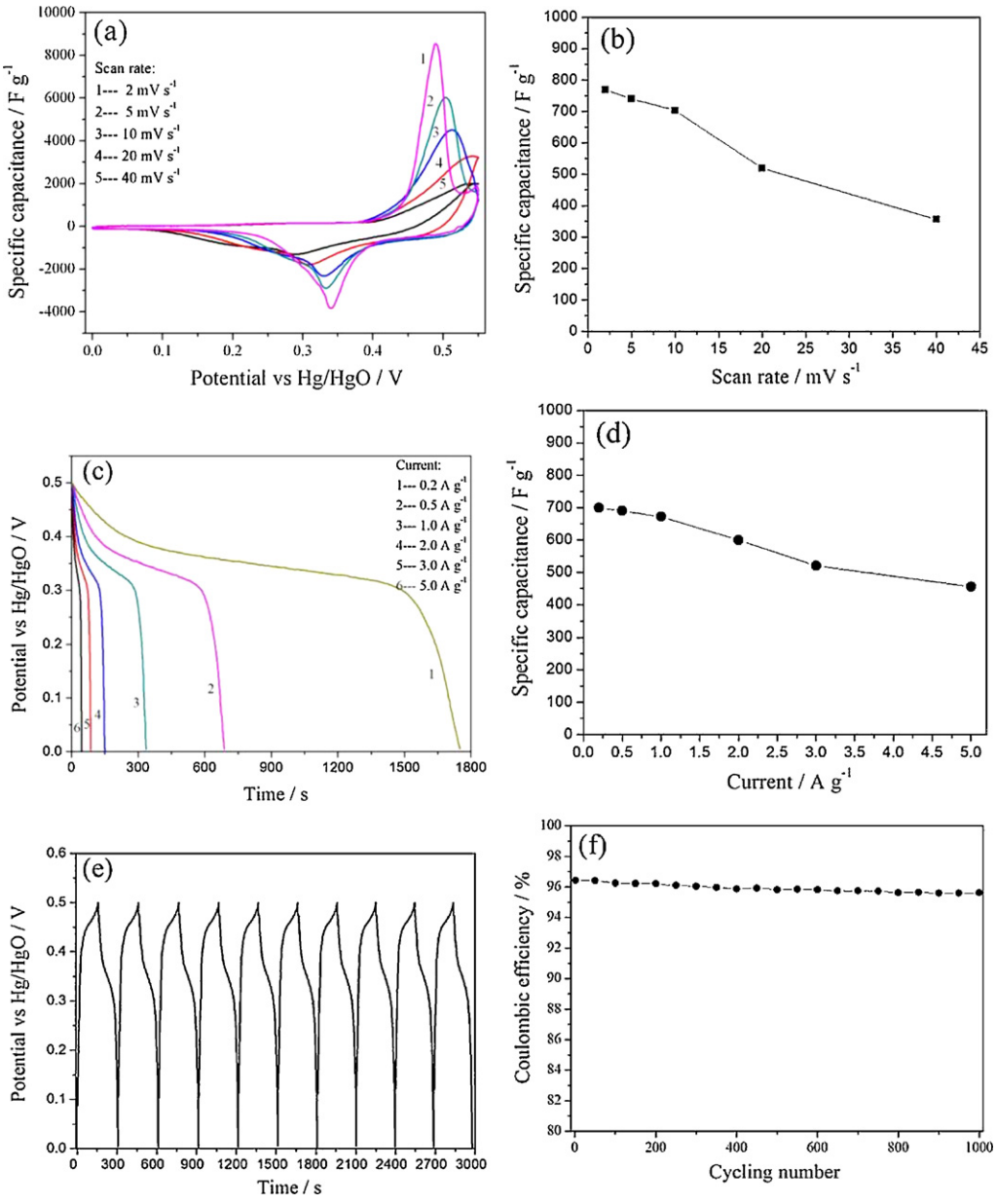


**Fig. 2.** Electrochemical performance of RG-O/NiO. (a) CV curves of RG-O/NiO at various scan rates. (b) Average specific capacitance of RG-O/NiO at various scan rates. (c) Galvanostatic discharge curves of RG-O/NiO at various discharge current densities. (d) Average specific capacitance of RG-O/NiO at various discharge current densities. (e) Galvanostatic charge and discharge curves of RG-O/NiO at a current density of 2 A $g^{-1}$. (f) Coulombic efficiency versus cycle number of RG-O/NiO at the current density of 2 A $g^{-1}$.

shown in Fig. 1c. For an isolated NiO nanosheet-based sphere-like particle (a 'microsphere'), the edge portion of the sphere-like structure is thinner than that of the center, and is comprised of sheet-like '2D' structures. From the HRTEM image of Fig. 1d, a single nanosheet in such microspheres shows a single-crystalline structure. The lattice spacing of 0.21 nm corresponds to the *d* spacing between adjacent (2 0 0) crystallographic planes of NiO crystal.

To measure the performance of the RG-O/NiO composite as electrode materials for supercapacitors, the composite was mixed with polytetrafluoroethylene (PTFE) in a weight ratio of 95:5 for preparing the working electrode, which is equivalent to a NiO:RG-O:PTFE ratio of 85.5:9.5:5. Carbon black (CB) or other carbonaceous materials can increase the conductivity of the electrode when preparing the electrode for electrochemical measurement. However, these additives can also lower the weight specific capacitance of the electrode. Carbon black or other additives were not added to the electrode in this work in comparison to the literatures [4,14].

Cyclic voltammograms (CVs) and galvanostatic charge/discharge measurements were carried out in a three-electrode system with an Hg/HgO (in 6 N KOH) reference electrode and 6 M KOH aqueous electrolyte. Fig. 2a shows CV curves of RG-O/NiO at various scan rates. As can be seen, CV curves exhibit a pair of redox peaks, signifying typical pseudocapacitor behavior. The redox current peaks corresponded to the reversible reactions of Ni(ii) ↔ Ni(iii). Considering the background signal to the Ni foam substrate was negligible (FS. 4), the redox current peaks were all attributed to the reversible redox process of NiO/NiOOH. The specific capacitance increases with decreasing scan rate. The specific capacitance of RG-O/NiO was calculated to be ~770 F $g^{-1}$ (based on mass of NiO, ~658 F $g^{-1}$ based on the total electrode mass) at a scan rate of 2 mV $s^{-1}$ (Fig. 2b), and ~356 F $g^{-1}$ even at

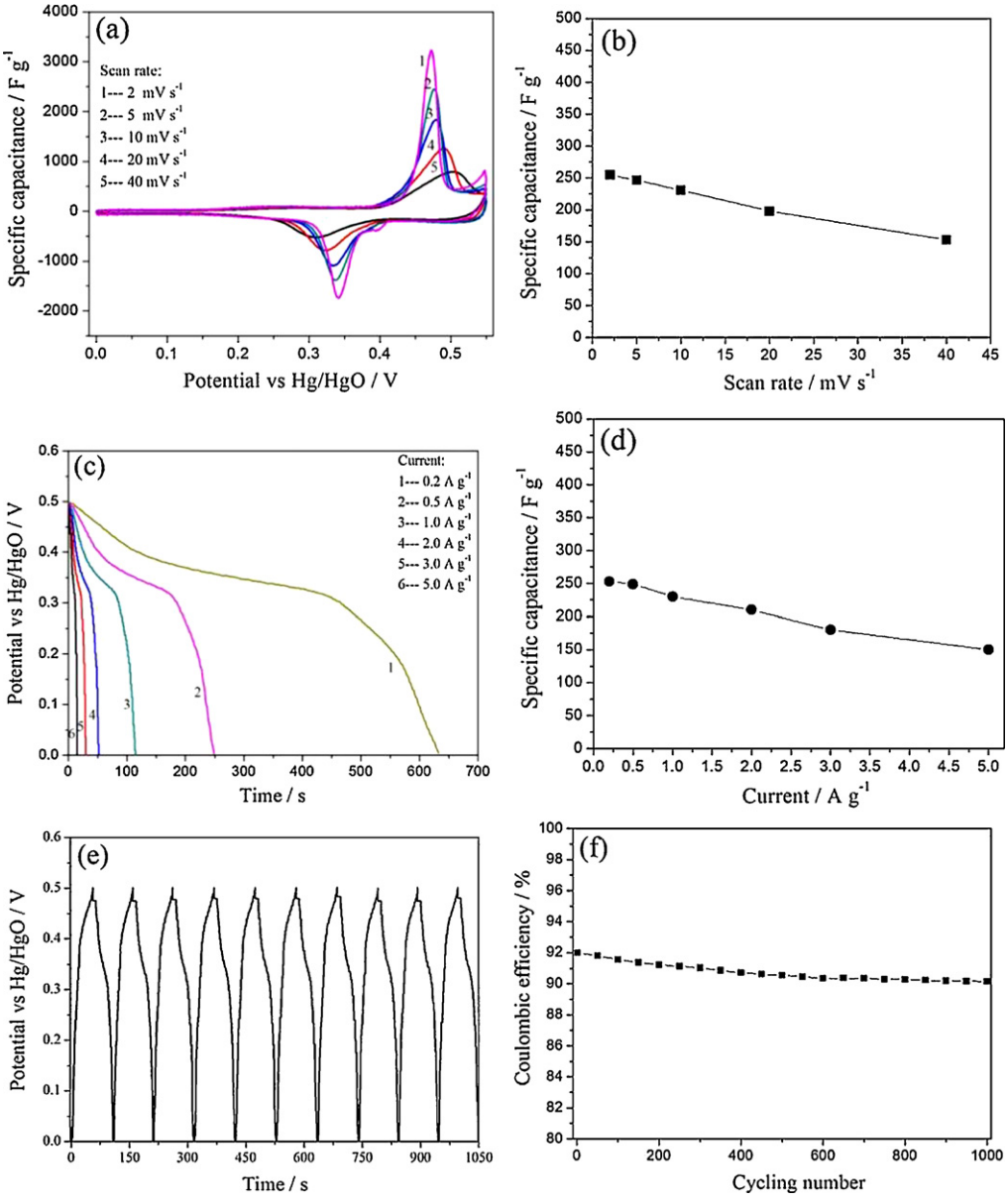


**Fig. 3.** Electrochemical performance of NiO. (a) CV curves of NiO at various scan rates. (b) Average specific capacitance of NiO at various scan rates. (c) Galvanostatic discharge curves of NiO at various discharge current densities. (d) Average specific capacitance of NiO at various discharge current densities. (e) Galvanostatic charge and discharge curves of NiO at a current density of 2 A $g^{-1}$. (f) Coulombic efficiency versus cycle number of NiO at a current density of 2 A $g^{-1}$.

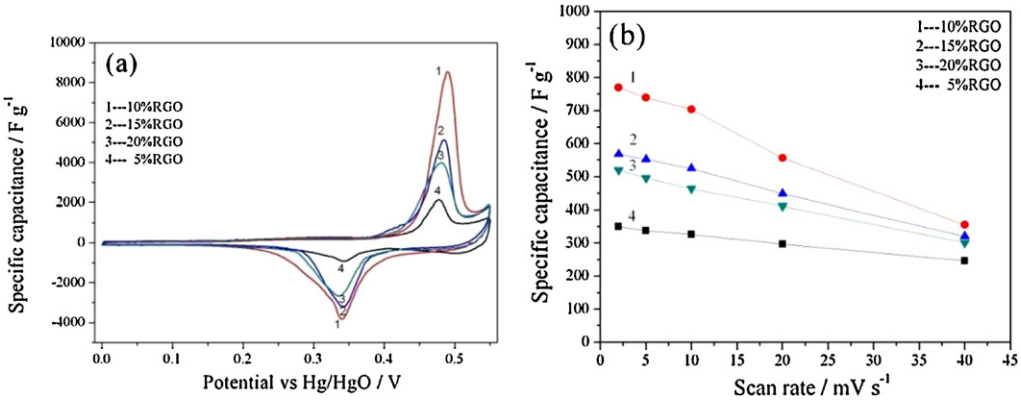


**Fig. 4.** Electrochemical performance of RG-O/NiO composites with different content of RG-O. (a) CV curves of RG-O/NiO composites at the scan rate of 2 mV $s^{-1}$. (b) Average specific capacitance of RG-O/NiO composites at various scan rates.

a higher scan rate of 40 mV $s^{-1}$ (based on mass of NiO). This is attributed to the different rate of alkali ion to go in and out the surface of the NiO particles and the surface of the RG-O platelets. At a low scan rate, the ions from electrolyte can access to almost all available sites of the electrode, leading to a complete insertion reaction, and thus resulting in a higher specific capacitance. Fig. 2c shows galvanostatic discharge curves of RG-O/NiO at various discharge current densities. The RG-O/NiO showed a specific capacitance of ~700 F $g^{-1}$ at a current density of 0.2 A $g^{-1}$. As the discharge current density increased, the specific capacitance decreased (Fig. 2d). The specific capacitance was still as high as 455 F $g^{-1}$ even at a higher current density of 5 A $g^{-1}$. Notably, the Columbic efficiency was more than 96% for each cycle during 1000 cycles (Fig. 2e and f), indicating that the high specific capacitance and remarkable rate capability of the RG-O/NiO composite for electrochemical supercapacitors.

In a comparison experiment, we synthesized NiO by the same method without any RG-O. Although the NiO particles had a morphology and crystallinity similar to those of the nanosheet-based NiO microspheres in the RG-O/NiO composite (see FS. 5), the electrochemical performance of NiO mixed physically with carbon black in the same mass weight ratio as the RG-O/NiO is much worse than that of RG-O/NiO composite. As shown in Fig. 3, the NiO exhibited much lower specific capacitance than the RG-O/NiO. The specific capacitance was ~255 F $g^{-1}$ (based on mass of NiO, ~218 F $g^{-1}$ based on the total electrode mass) at the scan rate of 2 mV $s^{-1}$, and ~153 F $g^{-1}$ at a high scan rate of 40 mV $s^{-1}$. The Coulombic efficiency was ~92% for each cycle during 1000 cycles, which is lower than that of RG-O/NiO.

For RG-O/NiO composite, NiO anchored on the surface of highly conducting RG-O exhibits excellent electrochemical capacitive characteristics, making it potential useful as electrode materials for high performance supercapacitors. Measured by the same CV or charge/discharge test, the RG-O/NiO composite shows higher stable specific capacitance than those previously reported, such as NiO [26] and NiO/carbonaceous materials [27,28]. The good electrochemical performance is attributed to the following advantages of the RG-O/NiO composite.

Because of covalent chemical bonding and Van der waals' force at oxygen-containing functional group sites and pristine region of the graphene, NiO particles are directly anchored on the surface of the RG-O platelets. The interaction between NiO particles and RG-O platelets is favorable to electron transport between NiO particles and RG-O platelets, which is a key to the high specific capacitance and rate stability of the RG-O/NiO composite. The particle-anchored, layered structure of RG-O/NiO has a highly effective surface contact with the electrolyte and a rich porous structure due to the spacing effect of NiO particles between adjacent RG-O platelets, shortening the insertion-desertion paths of ions through the graphene 3D network. Excellent electron transport from NiO particles to the underlying RG-O platelets leads to fast redox reactions at high scan rates or high current densities. For the physical mixture of presynthesized NiO and carbon black, the inferior electrochemical characteristics were mainly attributable to much less inter contact and bad conductivity between NiO particles and CB in the electrode. Therefore, the structural feature of RG-O/NiO composite ensures the effective utilization of both NiO and RG-O in the composite electrode.

In order to further understand the effect of RG-O content on the electrochemical performance of the RG-O/NiO, the composite with different RG-O content of 5, 10, 15, 20% were prepared. Fig. 4a shows the typical CV curves of RG-O/NiO electrodes measured in 6 M KOH at the scan rate of 2 mV $s^{-1}$ between 0.0 V and 0.55 V. The change of capacitive behavior is observed from the redox peak profiles relate to the NiO pseudocapacitive characteristics. The composites with 5, 10, 15 and 20% RG-O have 350, 770, 570 and 520 F $g^{-1}$ specific capacitance respectively. Among these, the composite with 10% RG-O has the highest specific capacitance of 770 F $g^{-1}$. At other scan rates for CV measurements (Fig. 4b), it is noted that the specific capacitance of the composite with 10% RG-O is also higher than that of the composites with 5, 15 and 20% RG-O respectively. As we know, when the NiO content is high, the specific capacitance of the RG-O/NiO composite comes mainly from Faradic reaction of NiO particles as $NiO + OH^- - e \rightarrow NiOOH$, and partially from electric-double-layer capacitance of RG-O (non-Faradic reaction). When the composite has a relatively good conductivity resulting from an optimum content of RG-O, the higher the content of NiO, the higher the specific capacitance. It is suitable for the composite with 10% RG-O and 90% NiO to have a good conductivity and high content of NiO, resulting in high specific capacitance of the as-prepared composite. We suggest that the composite with 10% RG-O can be used as high performance electrode materials for supercapacitors.

## 4. Conclusions

In summary, a simple approach is used to fabricate a reduced graphene oxide/nanosheet-based NiO microsphere composite in which NiO microspheres are uniformly decorated on the surface of reduced graphene oxide platelets. The composite exhibits enhanced electrode performance for supercapacitors with high specific capacitance, high electrochemical stability and high energy density. Considering the full utilization of the advantages of RG-O and NiO, the RG-O/NiO composite can be useful as electrode materials for high performance supercapacitors.

## Acknowledgements

This work was supported by the Natural Science Foundation of Hubei Province (No. 2011CDB161) and the Scientific Research Foundation for the Returned Overseas Chinese Scholars, State Education Ministry (SRF for ROCS, SEM).

## Appendix A. Supplementary data

Supplementary data associated with this article can be found, in the online version, at doi:10.1016/j.jpowsour.2011.11.055.

## References

[1] M.J. Allen, V.C. Tung, R.B. Kaner, Chem. Rev. 110 (2010) 132–145.
[2] A.S. Arico, P. Bruce, B. Scrosati, J.M. Tarascon, W. Van Schalkwijk, Nat. Mater. 4 (2005) 366–377.
[3] K.H. An, W.S. Kim, Y.S. Park, J.M. Moon, D.J. Bae, S.C. Lim, Y.S. Lee, Y.H. Lee, Adv. Funct. Mater. 11 (2001) 387–392.
[4] R.R. Bi, X.L. Wu, F.F. Cao, L.Y. Jiang, Y.G. Guo, L.J. Wan, J. Phys. Chem. C 114 (2010) 2448–2451.
[5] J. Gamby, P.L. Taberna, P. Simon, J.F. Fauvarque, M. Chesneau, J. Power Sources 101 (2001) 109–116.
[6] M. Kaempgen, C.K. Chan, J. Ma, Y. Cui, G. Gruner, Nano Lett. 9 (2009) 1872–1876.
[7] R. Kotz, M. Carlen, Electrochim. Acta 45 (2000) 2483–2498.
[8] A.K. Geim, Science 324 (2009) 1530–1534.
[9] K.S. Novoselov, A.K. Geim, S.V. Morozov, D. Jiang, Y. Zhang, S.V. Dubonos, I.V. Grigorieva, A.A. Firsov, Science 306 (2004) 666–669.
[10] M.D. Stoller, S.J. Park, Y.W. Zhu, J.H. An, R.S. Ruoff, Nano Lett. 8 (2008) 3498–3502.
[11] Y. Wang, Z.Q. Shi, Y. Huang, Y.F. Ma, C.Y. Wang, M.M. Chen, Y.S. Chen, J. Phys. Chem. C 113 (2009) 13103–13107.
[12] S. Park, R.S. Ruoff, Nat. Nanotechnol. 4 (2009) 217–224.
[13] H.C. Schniepp, J.-L. Li, M.J. McAllister, H. Sai, M. Herrera-Alonso, D.H. Adamson, R.K. Prud'homme, R. Car, D.A. Saville, I.A. Aksay, J. Phys. Chem. B 110 (2006) 8535–8539.
[14] G.M. An, P. Yu, M.J. Xiao, Z.M. Liu, Z.J. Miao, K.L. Ding, L.Q. Mao, Nanotechnology 19 (2008).
[15] Y.G. Guo, J.S. Hu, L.J. Wan, Adv. Mater. 20 (2008) 2878–2887.
[16] D. Grosso, G. Illia, E.L. Crepaldi, B. Charleux, C. Sanchez, Adv. Funct. Mater. 13 (2003) 37–42.
[17] F. Jiao, A.H. Hill, A. Harrison, A. Berko, A.V. Chadwick, P.G. Bruce, J. Am. Chem. Soc. 130 (2008) 5262–5266.
[18] K.C. Liu, M.A. Anderson, J. Electrochem. Soc. 143 (1996) 124–130.

[19] M.S. Wu, M.J. Wang, Electrochem. Solid-State Lett. 13 (2010) A1–A3.
[20] P. Lin, Q.J. She, B.L. Hong, X.A.J. Liu, Y.N. Shi, Z. Shi, M.S. Zheng, Q.F. Dong, J. Electrochem. Soc. 157 (2010) A818–A823.
[21] Y.L. Cao, J.M. Cao, M.B. Zheng, J.S. Liu, G.B. Ji, J. Solid State Chem. 180 (2007) 792–798.
[22] Y. Guo-hui, J. Zhao-hua, A. Aramata, G. Yun-zhi, Carbon 43 (2005) 2913–2917.
[23] Z.S. Wu, D.W. Wang, W. Ren, J. Zhao, G. Zhou, F. Li, H.M. Cheng, Adv. Funct. Mater. 20 (2010) 3595–3602.
[24] S. Chen, J. Zhu, X. Wu, Q. Han, X. Wang, ACS Nano 4 (2010) 2822–2830.
[25] W.S. Hummers, R.E. Offeman, J. Am. Chem. Soc. 80 (1958) 1339.
[26] S.K. Meher, P. Justin, G.R. Rao, Electrochim. Acta 55 (2010) 8388–8396.
[27] M.L. Zhang, Y.Z. Zheng, P. Gao, Mater. Res. Bull. 42 (2007) 1740–1747.
[28] J.M. Cao, Y.L. Cao, M.B. Zheng, J.S. Liu, G.B. Ji, J. Solid State Chem. 180 (2007) 792–798.